

Modeling ecosystem responses to prescribed fires in a phosphorus-enriched Everglades wetland: I. Phosphorus dynamics and cattail recovery

Hanqin Tian^{a,*}, Xiaofeng Xu^a, Shili Miao^b, Erik Sindhoj^{c,d}, Bray J. Beltran^a, Zhijian Pan^{a,e}

^a Ecosystem Dynamics and Global Ecology (EDGE) Laboratory, School of Forestry and Wildlife Sciences, Auburn University, Auburn, AL 36830 USA

^b South Florida Water Management District, Everglades Division, 3301 Gun Club Road, West Palm Beach, FL 33406, USA

^c Sceda Ecological Associates, 1486-E Skees Road, West Palm Beach, FL 33411, USA

^d Department of Crop Production Ecology, Swedish University of Agricultural Sciences, Box 7043, SE-75007 Uppsala, Sweden

^e Bio-Inspired Computing Group, Department of Computer Science, University of Maryland, College Park, MD 20742, USA

ARTICLE INFO

Article history:

Received 5 August 2009

Received in revised form

15 December 2009

Accepted 22 December 2009

Available online 22 January 2010

Keywords:

Cattail

Everglades

Fire

Phosphorus

Wetland Ecosystem Model (WEM)

ABSTRACT

We have developed and applied a process-based model, the Wetland Ecosystem Model (WEM), to evaluate the effects of a prescribed fire on the phosphorus (P) dynamics and cattail (*Typha domingensis*) growth in a P-enriched area in the Florida Everglades. The WEM couples major ecosystem processes including carbon (C), nitrogen (N) and P biogeochemical cycles, plant growth, hydrology, and fire disturbance. The model is used to assess the effects of a prescribed fire on P dynamics and cattail growth through dynamic interaction among four modules: fire, water chemistry, soil, and vegetation. The simulation results are in agreement with observed data including cattail above- and belowground biomass and dead mass, P concentration in surface-water, pore-water, and soil, and soil and water temperature. Cattail aboveground biomass reached the unburned level one year after burn; belowground biomass recovered to unburned level one and half years after the fire, however, dead mass did not completely reach unburned level two years after fires. The fire increased water and soil temperatures in the short term, while indirectly increasing the sensitivity of water and soil temperature post-fire response to air temperature by altering the energy exchange between air and water through a canopy gap created by fire. The fire also altered the P dynamics in surface-water and pore-water. A post-fire P pulse that lasted for less than one month was observed in surface-water. A similar P pulse, but in a small magnitude and a longer duration, was also observed in the pore-water total phosphorus (TP), and then came back to normal level after approximately three months. No significant changes in soil TP was observed during the study period. Meanwhile, no significant changes in water nutrients were observed downstream of the study plot. This finding indicated that the P-enriched wetlands in Everglades act as a buffer in regulating the P concentration in surface-water. Our study showed that the distance of fire effects on a 300 m × 300 m plot was less than 300 m downstream. Sensitivity analysis identified that the air temperature and hydrological conditions are two important driving factors which may alter the cattail community dynamics in response to prescribed fires. Similar to the field studies, this study provided evidences that fire played an important role in managing plant growth and P dynamics in the Florida Everglades.

© 2010 Elsevier B.V. All rights reserved.

1. Introduction

Wetland loss and degradation is a critical issue of great social and ecological significance around the world because it reduces the ability of wetlands to provide goods and services to humankind and to support biodiversity (Moser et al., 1996). Also, wetland degradation might substantially alter adjacent ecosystems and societies through shifting plant community structure (Finlayson and Rea,

1999), modifying local climate (Zedler, 2000), and/or changing water quantity and quality (Finlayson and Rea, 1999). Nutrient loading, especially nitrogen (N) and phosphorus (P), and its associated eutrophication, as well as the invasion of exotic species have been recognized as the major causes and features of wetland degradation (Moser et al., 1996; Finlayson and Rea, 1999; DeBusk et al., 2001). Therefore, the main goals of wetland restoration efforts are to reduce nutrient loading and to restore native vegetation (Zedler, 2000; Burns and McDonnell, 2003).

Regions of the Florida Everglades have experienced a serious degradation in the past half century, which derives from nutrient loading and altered hydrology. This has led to the deterioration of water quality and the expansion of cattail (*Typha domingensis*)

* Corresponding author. Tel.: +1 334 844 1059; fax: +1 334 844 1084.
E-mail address: tianhan@auburn.edu (H. Tian).

(Davis, 1994; Miao and Sklar, 1998; Miao and DeBusk, 1999). Several projects have been conducted to remove P from the inflow water into the Everglades; so a lower P concentration and a process of natural recovery of the impacted areas are expected (Miao and Carstenn, 2005; Li et al., 2009). However, in 2003, the Everglades Protection Area Tributary Basins Long Term Plan for Achieving Water Quality Goals (LTP) in the Everglades Protection Area anticipated that natural recovery would take too long (Burns and McDonnell, 2003) and alternative options for accelerating the recovery of the impacted areas need to be explored. Given the great amount of P sediment in the Everglades (DeBusk et al., 2001), active restoration of the degraded ecosystems may not be a good option because it may entail additional human disturbances and it might mobilize the accumulated phosphorus into more pristine areas downstream. Long-term solutions for accelerating the recovery of eutrophied wetlands have not been documented. Even though prescribed fire has been used to actively manage cattail dominated communities in other areas of Florida (Ponzio et al., 2004), little has been reported regarding the quantitative and long-term effects of fire or repeated fires on nutrient biogeochemistry in soils, water, vegetation, or the shifts in vegetation communities in areas of different nutrient enrichment.

In this context, a large field experiment, the Fire Project, was initiated to address such lack of knowledge on spatial and temporal responses to fires in the Everglades, and to assess whether multiple prescribed fires will cause a decline in cattail in the Water Conservation Area 2A (WCA-2A) (Miao and Carstenn, 2005). The underlying hypothesis of the Fire Project is that several consecutive fires may alter community structure through changing P dynamics. While the Fire Project is a large-scale ecological experiment using a whole-ecosystem approach, it is still temporally constrained. The experiment duration is four years, which allowed for only two prescribed fires to be conducted. To cope with such temporal constraints and evaluate the long-term responses of cattail to fires, alternative approaches, such as computational simulation, need to be explored.

In the past decades, several models have been developed to study the biogeochemical cycles of carbon (C), N and P in wetland ecosystems. For example, the Everglades Landscape Model (ELM) was specifically created to study the Everglades wetland ecosystem (Fitz and Tribble, 2006). In the ELM model, however, the plant growth component is not robust enough to simulate the fire effects on different plant tissues. This is because the method used to describe the major processes for macrophyte growth in ELM is purely empirical, and has no allocation for different plant tissues, which may cause biases in simulating the community shift in response to fires and associated P dynamics. The Wetland version of DeNitrification-DeComposition (Wetland-DNDC) model is a wetland ecosystem model developed to simulate the biogeochemical processes in forested wetlands (Zhang et al., 2002). However, the water balance and P dynamics are not included in the system (Zhang et al., 2002). Therefore, ELM and Wetland-DNDC are not robust enough to effectively simulate the effects of P loading on the plant community shift, which is the ultimate goal of the Fire Project (Miao and Carstenn, 2005). There are a number of other models which are not suitable for the Fire Project due to the lack of one or several sub-models. For example, Wang and Mitsch's (2000) phosphorus model cannot simulate plant growth and nitrogen processes; Chen and Twilley's (1999) mangrove nutrient model does not incorporate the biomass production; Richardson et al.'s (1996) predictive models only consider the phosphorus retention in wetlands while does not simulate the plant growth. Wynn and Liehr's (2001) dynamic compartmental simulation model does not consider the phosphorus processes. A new wetland model coupling carbon, nitrogen and phosphorus dynamics, plant growth, hydro-

logical and thermal dynamics, and fire effect, targeting Everglades' wetland, is needed.

A biogeochemical model with artificial evolution of ecosystem responses to prescribed fires in WCA-2A, Everglades FL, can provide at least the following advantages: (1) a longer temporal scale can be easily incorporated, (2) "what-if" questions can also be easily assessed, (3) it becomes possible to computationally forecast how the cattail ecosystem may respond to future decreased nutrient loading and fire management, and (4) it becomes possible to control all the parameters and environments under question which is simply impossible at the physical experimental level. For these reasons, we investigated the possibility of establishing a computational wetland ecosystem model that can determine if prescribed fire will accelerate the recovery of the degraded areas within the Everglades ecosystem.

The objectives of this study are: (1) to develop a process-based biogeochemical wetland model; (2) to test the robustness of the newly built model in simulating phosphorus dynamics in water and plant growth in the Florida Everglades' P-enriched area; (3) to examine the optimal controls of parameters and environmental factors for this model by conducting a sensitivity analysis; and (4) to apply the model to evaluate the effects of a prescribed fire on the phosphorus dynamics and cattail recovery.

2. Materials and methods

2.1. Model development

To address the objectives of the Fire Project, the Wetland Ecosystem Model was developed to evaluate and predict the effects of fire on plant and P dynamics in a wetland ecosystem (Tian and Xu, 2007; Xu et al., 2008). The model was compartmentalized into vegetation, soil, water chemistry and fire mentioned previously (Fig. 1). Briefly, the vegetation module simulates plant growth, C cycling, and nutrient uptake and accumulation in plants. The soil module simulates the dynamics of C, N and P in soil as well as other physical and chemical properties (e.g. soil temperature). The water chemistry module is used for simulating the water budget consisting of water input from rainfall and upstream inflow; and water losses from evapo-transpiration (ET) and downstream outflow. The fire module considers biomass burning and nutrient (mainly as ash) deposition into the ecosystem as the key nutrient recycling processes, and the diffusion and downwind transport of ash as a main nutrient export processes from the experimental plot.

The WEM has a daily time step; however, some physiological and hydrological processes are updated every 30 min, e.g., heat transfer between different water layers, and nutrient ion diffusion in the water matrix. The daily time step was chosen because the dynamics of ecosystem and P in the system can be easily captured and described computationally at this scale. The WEM was developed using C++ programming language.

2.1.1. Fire module

In the fire module, the fire effects on above- and below-ground, biomass and dead mass are simulated. During burning, large fractions of the aboveground biomass and dead mass are consumed. The fraction of biomass and dead mass that remains above the water surface is calculated from the following equation:

$$F_{\text{Fire}} = 0 \quad \text{WT} > H_{\text{max}}$$

$$F_{\text{Fire}} = 1.0 - \frac{2.0 \times \text{WT}}{\text{WT} + H_{\text{max}}} \quad \text{WT} > 0 \text{ and } \text{WT} < H_{\text{max}}$$

$$F_{\text{Fire}} = 1 \quad \text{WT} \leq 0$$

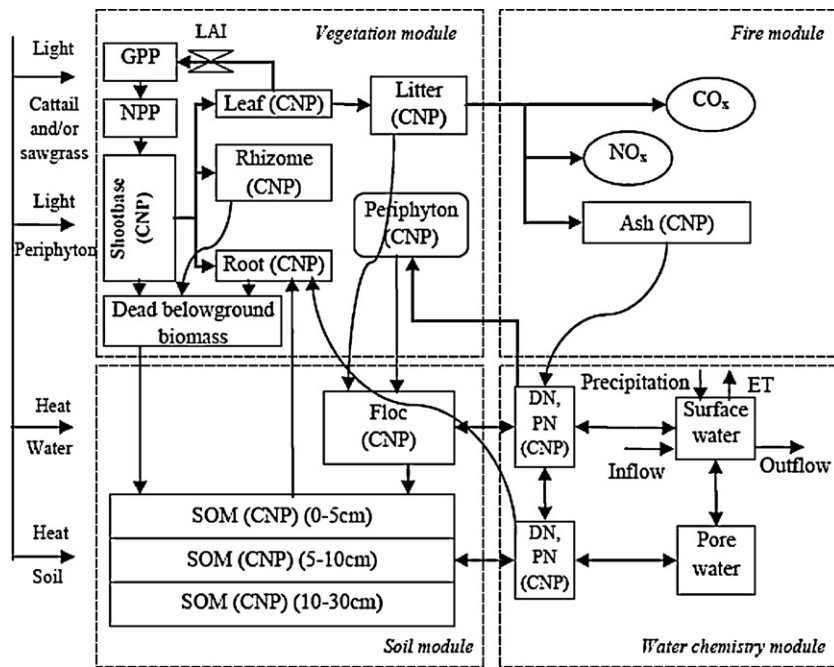


Fig. 1. Conceptual model of the wetland ecosystem model (WEM). The model has four interacting modules: vegetation module, soil module (C, N, and P), water chemistry module, and fire module. The dashed line separates the modules, and arrows represent material and energy flow.

$$\text{Litter}_{\text{Fire}} = F_{\text{Fire}}$$

$$\text{Leaf}_{\text{Fire}} = (F_{\text{Fire}})^2$$

where F_{Fire} (unit-less) is the fraction of biomass and dead mass above the water surface that burned, WT (m) is the water depth, and H_{max} (m) is the maximum plant height. The WEM assumes a single fire consumes less biomass than dead mass, so the F_{fire} for biomass is different from that for dead mass. $\text{Litter}_{\text{Fire}}$ is the fire effect on litter; and $\text{Leaf}_{\text{Fire}}$ is the fire effect on living leaves. If water depth falls below soil surface, fire will influence all the aboveground plant biomass and dead mass, and may consume the accumulated organic matter in soil; this is detrimental and will be prevented in any prescribed fires.

Fires do not consume all aboveground biomass due to its relatively high water content. Nevertheless, the heat scorches a large fraction of the aboveground biomass which is then converted to dead mass in subsequent days after the burn. In addition, fires cannot consume all the dead mass, so a portion of this material will remain in the system. All the burned biomass and dead mass forms gases such as carbon dioxide (CO_2) and nitrogen oxides (N_xO_x), or C, N and P ash according to the fire efficiency:

$$\text{Gas} = F_{\text{Fire}} \times \text{FireEff}_{\text{c,n,p}} \times \text{Biomass}_{\text{c,n,p}} \times \text{FireInten}$$

$$\text{Ash} = \text{Biomass}_{\text{c,n,p}} \times \text{FireInten} \times F_{\text{Fire}} - \text{Gas}$$

where Gas is the gaseous form of C and N which will leave the system (WEM assumes no gas form for P); FireInten is the fire intensity which is used to define the strength of specific fire; FireEff_{c,n,p} is the fire efficiency of biomass C, N, and P (g C/g C; g N/g N; g P/g P), and it represents the fraction of biomass or dead mass consumed by a fire whose intensity is 1; and Biomass_{c,n,p} is the C, N and P content in the aboveground biomass or dead mass (g C, N, P/m²). Ash is the ash from burned biomass or dead mass (g C, N/m²). The C and N gases remain in the atmosphere, and portions of C, N, and P ash may return back to the system as particulate organic nutrient pools in

the surface-water. A portion of the ash leaves the system through downwind and diffusion transport.

2.1.2. Water chemistry module

The water chemistry module primarily simulates the water budget and nutrient dynamics in water. The water budget component includes all major hydrological processes in the Everglades (rainfall, inflow, outflow and ET). Rainfall directly enters the surface-water pool. Inflow, outflow, and ET occur in the surface-water pool; the pore water pool may support ET and accept rainfall if no surface water exists. Various nutrient forms exist in each water pool and link to other modules through nutrient cycling. For example, emergent plants take up nutrients from pore-water, and periphyton only takes up nutrient from surface water. The different forms of nutrients are interchangeable; one form may convert to or from another form. For example, particulate organic phosphorus (POP) may dissolve and enter the dissolved organic phosphorus (DOP) pool, and the DOP may be mineralized and enter the dissolved inorganic phosphorus (DIP) pool.

2.1.2.1. Hydrological elements.

2.1.2.1.1. Rainfall. Daily rainfall directly enters the surface-water pool as one of the main water fluxes. As high temporal resolution rainfall data were available for the area, the effects of seasonal dynamics of rainfall on the water budget are included in the WEM model.

2.1.2.1.2. Evapo-transpiration. WEM simulates ET based on incoming solar energy, following Abtew's equation that has been validated in comparison to ET measurements from the Everglades (Abtew, 2005)

$$\text{ET} = K \frac{R_s}{\lambda}$$

where ET is daily ET (m/d). R_s is solar radiation (MJ/m²/d), λ is the latent heat of vaporization (MJ/kg), and K is an empirical coefficient for the solar energy used for ET (0.53). If surface water does not exist, ET is supported by the first 5 cm of pore-water.

2.1.2.1.3. Inflow and outflow. Surface-water inflow is input as model-driven data; either water depth or outflow must be provided. Based on the law of conservation of mass, outflow is calculated if water depth is provided. If water depth is not available, the outflow rate must be provided.

2.1.2.1.4. Change in water storage. The change in water storage is calculated using the following equation

$$\Delta S = P + Q_{in} - ET - Q_{out}$$

where ΔS is the net change in the water volume of the system (m^3/m^2); P is rainfall (m^3/m^2); Q_{in} is inflow (m^3/m^2); and Q_{out} is outflow (m^3/m^2).

2.1.2.1.5. Water depth. Water depth is expressed as the actual surface water body above soil surface. Considering the high rainfall and abundant inflow to the Everglades, the WEM assumes that the water depth in the Everglades does not fall to 5 cm below the soil surface. Water depth is tightly linked to soil processes because it influences the downward transfer of heat. It also influences fire effects on aboveground biomass and dead mass because these will not burn when they are under water (see Section 2.1.1). Water depth might alter post-fire plant growth through changing nutrient dynamics and local hydrology.

2.1.2.2. Water chemistry components. Water in the system contains several nutrient forms which support plants and periphyton. Major nutrient pools are dissolved nutrient (DN) and/or particulate nutrient (PN). The DN pool exists mainly as dissolved organic nitrogen (DON), DOP, dissolved inorganic N (DIN such as NO_3^- , NH_4^+) and DIP (mainly as phosphate [PO_4^{3+}]). The PN pool exists mainly as particulate organic N (PON) and POP.

2.1.2.2.1. Carbon. Carbon in water exists mainly as particulate organic C (POC) and dissolved organic C (DOC). Because N and P limit aquatic photosynthesis more frequently than does inorganic carbon (Wetzel, 2001), WEM does not simulate inorganic C. POC mainly comes from aboveground dead mass and floc. Portions of POC are mineralized to form CO_2 , while some will dissolve and enter the DOC pool. A portion of DOC is also mineralized and leaves the system as CO_2 , while the remaining portion of DOC accumulates in the system as soil organic C. All these C flows between pools are described as first-order kinetics. Particulate organic C and DOC may leave the system in association with water outflow.

2.1.2.2.2. Phosphorus. Phosphorus in water exists not only as POP and DOP, but also as DIP. POP mainly comes from aboveground dead mass and floc. A portion of POP will be mineralized to form DIP, while some will dissolve and enter the DOP pool. A fraction of DOP and POP accumulates in soil organic matter (SOM) while portions of DIP, POP, and DOP may leave the system in association with water outflow. All these P flows between pools are described as first-order kinetics. Phosphorus input occurs in two ways, P deposition and inflow. Daily deposition and inflow data are provided by users. WEM requires the daily deposition information to calculate the P balance in system. Phosphorus inflow enters the surface nutrient pools through water inflow. Phosphorus loss in WEM occurs mainly through outflow. The outflow rate is inputted by the user or is calculated based on water inflow and water depth.

2.1.2.2.3. Nitrogen. Similar to P, N in water exists in forms of PON, DON and DIN including nitrate (NO_3^-) and ammonium (NH_4^+). PON mainly comes from aboveground dead mass and floc. Portions of PON mineralize to form DIN, and some dissolves and enters the DON pool. A portion of DON and PON accumulates into SOM. Portions of DIN, PON, and DON also may leave the system in association with water outflow. All these N flows between pools are described as first-order kinetics. The current version of WEM does not simulate the processes of biological N fixation by symbiosis. Daily deposition and inflow data are provided by the user.

The daily N deposition (including both NO_3^- and NH_4^+ in wet and dry deposition) information is used to calculate the N balance in the system. Nutrients enter their corresponding N pools in water directly. Nitrogen inflow is processed similarly to N deposition; but it only occurs in association with water inflow. WEM also does not consider nitrification and denitrification processes. Nitrogen loss mainly occurs through water outflow in inorganic or organic forms.

2.1.3. Soil module

The soil module is the most complex component in the WEM. It simulates soil temperature dynamics and nutrient cycling along the soil profile. The WEM includes a nutrient layer that is important in the Everglades, the floc layer, which is located immediately above the soil surface. Floc, the intermediate layer between aboveground dead mass and SOM, is highly nutrient enriched and links plants, surface-water and soil together. It functions like a transitional nutrient storage, linking C, N, and P cycling among cattail, water and soil components.

2.1.3.1. Soil temperature. Soil temperature is calculated based on heat transfer along the soil/peat profile, which has been used by previous studies (Bonan, 1996; Granberg et al., 1999). The heat storage in an individual soil layer determines its temperature based on its physical and chemical properties. The soil/peat profile is divided into three layers, 0–5 cm, 5–10 cm, and 10–30 cm.

$$\frac{\partial(CT)}{\partial t} = \frac{\partial(\alpha(\partial T/\partial z))}{\partial z}$$

where t is time (hour), z is depth (cm), C is volumetric heat capacity of peat soil ($\text{J}/\text{cm}^3/\text{K}$), T is current soil/peat temperature (K), and α is the thermal conductivity ($\text{J}/\text{s}^2/\text{cm}/\text{K}$). The boundary temperature for the soil bottom is determined based on long-term observations.

2.1.3.2. Soil nutrient dynamics. Soil nutrients in the WEM are stored in three pools characterized by their decomposition rates: labile, intermediate, and recalcitrant. The decomposition rate for each soil nutrient pool was calibrated to literature values or field data. All mineralization processes follow first-order kinetics with k as the decomposition coefficient. The C released from the decomposition of these pools comprises heterotrophic respiration. Associated N and P mineralization is determined by the C:N, and C:P ratios of the individual pool.

2.1.3.2.1. Phosphorus dynamics. Phosphorus in soil is tightly coupled with soil carbon in different pools. The P flow between soil nutrient pools is calculated based on C:P ratios of the individual pool. Each SOM pool has an optimal C:P ratio; when C is lost from the detrital pool due to decomposition, the coupled P will be released (mineralized PO_4^{3-}), and enter the water nutrient pool.

2.1.3.2.2. Nitrogen dynamics. Similar to P, the N dynamics in WEM are coupled with C. Nitrogen mineralization is coupled with SOM decomposition. Each SOM pool has an optimal C:N ratio; when C is lost from a detrital pool due to decomposition, the coupled N is released (mineralized NH_4^+), and enter the water nutrient pool.

2.1.3.3. Litter and soil pools. WEM considers aboveground dead mass as the litter pools including labile, intermediate, and recalcitrant pools. Litter pools undergo chemical degradation at different rates, producing a connected series of aboveground dead mass and SOM pools. Carbon flows from one pool to another and CO_2 is released during this process. The magnitude of C fluxes depends on the size of aboveground dead mass and SOM pools and their decomposition rate constants. The decomposition rate for aboveground dead mass depends on air temperature, and the decomposition rate for SOM pools depends on soil temperature:

$$k_i = \text{tnr}_i \times k_t$$

where k_i is the decomposition rate constant of the detrital pool i ; tnr_i is the maximum turnover rate of the detrital pool i ; and k_t is the temperature scalar. WEM assumes that the temperature effects on decomposition rate constants are positively related to air/soil temperature (T_k) according to the formula:

$$k_t = \exp \left[308.56 \times \left(\frac{1}{71.02} - \frac{1}{T_k - 227.13} \right) \right]$$

The total C (TC) lost from the detrital pool i due to decomposition is calculated as:

$$\text{DecomLossC}_i = k_i \times \text{DecomDC}_i$$

where DecomDC_i (g C/m²/day) is the C pool size in the detrital pool i . A fraction of the decomposed C is released to the atmosphere as heterotrophic respiration, while the remaining fraction of decomposed C is transferred into another pool which has a lower decomposition rate (Fig. 1).

The CO₂ released due to the decomposition of pool i (Rh_i) is estimated as:

$$\text{Rh}_i = \text{krh}_i \times k_i \times \text{DecomDC}_i$$

where krh_i is a parameter that represents the fraction of C lost through heterotrophic respiration during the decomposition of the C pool i . For the recalcitrant SOM pool, $\text{krh} = 1$.

The C transferred from the detrital pool i into another detrital pool with a slower decomposition rate is calculated as:

$$\text{TransC}_i = (1 - \text{krh}_i) \times k_i \times \text{DecomDC}_i$$

The C balance of pool i is determined by its loss through decomposition and C flow into other pools. The ecosystem daily soil heterotrophic respiration rate (Rh_{soil} , in g C/m²/day) is the sum of all CO₂ released during decomposition of the detrital pools. The floc formation from aboveground dead mass, and floc loss through decomposition follow first-order kinetics with different rate coefficients set by the users.

2.1.4. Vegetation module

The vegetation module is the fundamental component for C cycling in the system, which is the primary carrier of nutrients. The plant growth module simulates the dynamics of plant biomass under various conditions. There are three primary elements (C, N, and P) which are continuously flowing in the system, and each element independently forms a cycle. In WEM, these elements are coupled in many ways, such as photosynthesis, leaf C:N:P stoichiometry, element allocation, soil decomposition, etc. The C, N, and P processes are independently listed and some interactions are highlighted below.

2.1.4.1. Carbon processes. Carbon processes considered in the WEM mainly include gross primary production (GPP, in g C/m²/day), allocation of the photosynthetic products, and autotrophic respiration of each cattail tissue. Carbon is gained through GPP, and is lost through autotrophic respiration; the balance of which forms net primary production (NPP). Changes in plant biomass including leaf, root, shootbase, and rhizome depend on the net C budgets of these tissues. Root exudation is also simulated in the WEM because it is one of the major processes which release plant carbon to DOC pools in wetland ecosystem (Reddy and DeLaune, 2008). Plant mortality is another important process which is used to simulate the natural death of cattail at daily time step. The dead cattail biomass will go directly to above- or below-ground dead mass.

2.1.4.1.1. GPP. The photosynthesis sub-model in WEM estimates the net C assimilation rate, leaf daytime maintenance respiration rate, and GPP. The photosynthesis rate is calculated at

the leaf level and multiplied by leaf area index (LAI) to scale up to ecosystem-level GPP.

Photosynthesis is based on the models of Farquahar et al. (1980) and Collatz et al. (1991). At the canopy level, leaf N concentration exerts impacts on photosynthesis. Leaf photosynthesis (A), the leaf CO₂ assimilation rate ($\mu\text{mol CO}_2/\text{m}^2/\text{s}$), is regulated by the minimum of RuBP carboxylase (Rubisco) limited rate of carboxylation (w_c), the light limited rate of carboxylation (w_j), or the export limited rate of carboxylation (w_e) (Bonan, 1996):

$$A = \min(w_c, w_j, w_e)$$

$$w_c = \frac{(c_i - \Gamma^*)V_{\text{max}}}{c_i + K_c(1 + o_i/K_o)}$$

$$w_j = \frac{(c_i - \Gamma^*)4.6\phi\alpha}{c_i + 2\Gamma^*}$$

$$w_e = 0.5V_{\text{max}}$$

where c_i is the internal leaf CO₂ concentration (Pa); o_i is the internal leaf O₂ concentration (Pa); Γ^* is the CO₂ compensation point (Pa); K_c and K_o are the Michaelis-Menten constants for CO₂ and O₂, respectively; α is the quantum efficiency; ϕ is the absorbed photosynthetically active radiation (PAR) (W m^{-2}); and V_{max} is the maximum rate of carboxylation that varies with temperature, foliage N concentration, and air temperature (Bonan, 1996):

$$V_{\text{max}} = V_{\text{max}25} a_{v\text{max}}^{(T_{\text{day}} - 25/10)} f(N) f(T_{\text{day}})$$

where $V_{\text{max}25}$ is V_{max} at 25 °C, $a_{v\text{max}}$ is a temperature sensitivity parameter; and $f(T_{\text{day}})$ is a function of temperature related metabolic processes

$$f(T_{\text{day}}) = \frac{(T_{\text{day}} - T_{\text{min}})(T_{\text{day}} - T_{\text{max}})}{(T_{\text{day}} - T_{\text{min}})(T_{\text{day}} - T_{\text{max}}) - (T_{\text{day}} - T_{\text{opt}})(T_{\text{day}} - T_{\text{opt}})}$$

where the T_{day} is the average daily temperature; T_{min} is minimum temperature for photosynthesis; T_{max} is the maximum temperature for photosynthesis; T_{opt} is the optimal temperature for photosynthesis.

The $f(N)$ is used to adjust the rate of photosynthesis based on foliage N:

$$f(N) = \min \left(\frac{50 \times N_{\text{leaf}} \times (1/C_{\text{leaf}})}{N_{\text{leaf,opt}}}, 1 \right)$$

where N_{leaf} is the foliar N concentration; C_{leaf} is the foliar C concentration; $N_{\text{leaf,opt}}$ is the optimal N concentration in leaf for photosynthesis.

GPP, estimated by scaling up the C assimilation from leaf level to ecosystem-level, is calculated using

$$\text{GPP} = \text{Rd} + \text{LAI} \times A \times 12.01 \times 10^{-6}$$

where GPP is gross primary productivity of the total canopy; Rd (mol C/s/m^2 leaf area) is the leaf daytime maintenance respiration rate; and 12.01×10^{-6} converts the unit from $\mu\text{mol C}$ to gram of C.

2.1.4.1.2. Allocation. In the WEM, the carbon in GPP will be allocated to each tissue after photosynthesis. The leaves have the highest priority to get carbon, so a portion of the fixed carbon will go to leaves. After that the remained photosynthetic product will be allocated to other tissues based on the parameters set by users.

$$\text{GPP}_{\text{leaf}} = \text{GPP} \times \left(\frac{\text{MaxLeafC} - \text{LeafC}}{\text{MaxLeafC}} \times \text{Slope} + \text{Inter} \right)$$

$\text{GPP}_i = \text{Allocation}_i \times (\text{GPP} - \text{GPP}_{\text{leaf}})$ where GPP_{leaf} is the carbon in GPP which will be allocated to leaf (g C/m²/day); MaxleafC is the maximum carbon for cattail leaf (g C/m²/day); LeafC is the carbon content in cattail leaves (g C/m²/day); slope and inter are two parameters set by user; GPP_i is the carbon in GPP which will

be allocated to tissue i (Rhizome, Shootbase, Root) ($\text{g C/m}^2/\text{day}$); Allocation_i is the parameters set by user for specific tissue.

2.1.4.1.3. Autotrophic respiration. The WEM estimates two types of respiration: maintenance respiration (Mr , in $\text{g C/m}^2/\text{day}$) and growth respiration (Gr , in $\text{g C/m}^2/\text{day}$). Mr is calculated first. If GPP is larger than Mr , then Gr is calculated by assuming that all GPP (i.e. the TC assimilated by the leaves in a day) that is not consumed by Mr is used to construct new tissue. It is assumed that 20% of the C (used to build new tissue) is released back into the atmosphere as Gr (Raich et al., 1991; Tian et al., 2005, 2010); the other 80% represents NPP. Therefore:

$$\text{Gr} = \text{MAX}(0.2 \times (\text{GPP} - \text{Mr}), 0)$$

$$\text{NPP} = \text{MAX}(0.8 \times (\text{GPP} - \text{Mr}), 0)$$

Maintenance respiration is positively correlated with temperature and biomass C content (Raich et al., 1991). The following equation is used to calculate the Mr for leaf, shootbase, rhizome, and roots:

$$\text{Mr}_i = \text{respcoeff} \times C_i \times \exp(0.0693 \times T)$$

where i denotes the different pools (leaf, shootbase, rhizome or roots); Mr_i ($\text{g/m}^2/\text{day}$) is the maintenance respiration of i th pool; C_i (g C/m^2) is the carbon content of the i th pool; respcoeff is the specific plant functional type respiration coefficient; and T is the daily temperature as air temperature (T_{avg}) for aboveground biomass, and soil temperature (T_{soil}) for belowground biomass. Finally, the total daily maintenance respired C is deducted from the individual plant C pool.

2.1.4.1.4. Root exudation. Root exudation (REC) is one of the major contributions to SOM from plants; it mainly included ethanol, carbohydrates, and amino acids (Reddy and DeLaune, 2008):

$$\text{REC} = \exp(-10) \times \text{TC}$$

where REC is the C released from fine roots ($\text{g C/m}^2/\text{day}$), a fraction of root biomass; and TC is the C content of fine roots (g C/m^2). The root exudation C enters the water DOC pool.

2.1.4.2. Nitrogen processes. In the WEM, N processes are intimately coupled to C processes by setting an optimized value and a range for C:N ratio for the different biomass pools. When the amount of stored N is insufficient to maintain the optimal plant C:N ratio, plant growth is inhibited, and excess C is stored in the C storage pool. Likewise, when N is surplus excess N is stored in the N storage pool. The N uptake rate of vegetation is affected by plant's overall C:N ratio, providing a feedback mechanism. Several important N processes in the WEM model are described in detail below.

2.1.4.2.1. Nitrogen uptake. Inorganic N in water and soil is taken up by plants to support their physiological functions and it follows the Michaelis-Menten equation, in which the N half-saturation coefficient and maximum uptake rate are set by the user

$$U_n = \frac{U_{\text{max}} \times \text{DIN}}{\text{DIN} + U_{1/2}}$$

where U_n is the plant N uptake rate ($\text{g N/m}^2/\text{day}$); U_{max} is maximum plant N uptake rate ($\text{g N/m}^2/\text{day}$); DIN is the concentration of dissolved inorganic N in the environment (g N/m^2); and $U_{1/2}$ is the N half-saturation coefficient (g N/m^2).

2.1.4.2.2. Nitrogen resorption. Portions of N in senescing leaves are translocated to the storage pool, shootbase, for use in the following growing season. The proportion of N resorbed depends on the parameters set by users. Re-sorbed N is added to the storage N pool.

2.1.4.2.3. Nitrogen allocation. After N is absorbed by plant roots, portions of it are transported to other tissues for physiological functions. This allocation depends on the N demand of each tissue. In WEM, the Deficiency Nitrogen Index (DNI) is defined to express the N demand of each tissue

$$\text{DNI}_i = \ln \left(\frac{C_i/N_i}{\text{CN}_{\text{opt}}} \right) + 0.5$$

where DNI_i is the deficiency N index, C_i is the C content of tissue i (g C/m^2), N_i is N content of tissue i (g N/m^2), and CN_{opt} is optimal C:N ratio of tissue i (g C/g N). The WEM is programmed to set the DNI in the range of 0 to 1, after the initial calculation. If the initial result is less than 0, the WEM sets it as 0; and if it is larger than 1, the WEM sets it as 1. Nitrogen taken up by plants is allocated to each tissue according to its DNI. If DNI is too large, indicating higher N deficiency, more N will be allocated to that tissue, and *vice versa*.

2.1.4.2.4. Root exudation.

$$\text{REN} = \exp(-10) \times (\text{TN} - \text{TC}/R_{\text{CN}})$$

The REN is root exudation N from fine roots ($\text{g N/m}^2/\text{day}$); and TN and TC are N and C content (g N/m^2 ; g C/m^2), and R_{CN} is the optimal C:N ratio of fine roots (g C/g N). Nitrogen exudates dissolve in water and enter the DON pool.

2.1.4.3. Phosphorus processes. Similar to the N processes, WEM considers P processes as P uptake, P allocation, P resorption, and root exudation. The equations used for P processes are the same as those in N cycles with different parameters.

2.2. Data preparation

Data for the model simulation included climatic conditions (air temperature, rainfall, solar radiation, and PAR), inflow water and associated nutrient dynamics. These data were retrieved from the South Florida Water Management's DBHYDRO database (http://my.sfwmd.gov/dbhydroplsqli/show_dbkey_info.main_menu). All climate data were measured at site WCA2F4, which is less than 5 km away from our experimental plots in the WCA-2A. Reference water level data were measured at site WCA2E1, which is approximately 10 km away from the burned plot. The daily reference water level data were used to as a control for the water depth dynamics in the simulations. Both N and P depositions were assumed to be invariable throughout the study. Based on a synthesis of field observations from Florida Lakes (Brezonik and Pollman, 1999), the N deposition was set at $0.002 \text{ g N/m}^2/\text{day}$, and the P deposition was set at $0.00015 \text{ g P/m}^2/\text{day}$. Other model data including vegetation, water chemistry and soil parameters were obtained from the Fire Project or the literature (Tables 1 and 2).

2.3. Model initialization, parameterization, and calibration

The initial conditions and major parameters used in the model simulation are given in Tables 1 and 2. First, we set the WEM to the initial state described in Table 1. The WEM simulation was then set up with the additional input data, and the major parameters were fine-tuned during the model calibration process (Table 2).

The WEM was calibrated using field data from the unburned control plot monitored by the Fire Project, and then validated against field data from the burned plot (Table 3). The detailed information of unburned site (H1) which is used for model calibration could be found in Table 3. Two scenarios were modeled: a burned scenario that simulated the ecosystem dynamics after a fire on July 25, 2006; and, an unburned scenario that assumed no fire during

Table 1
Initial conditions for the WEM in simulation of a highly P-enriched Everglades wetland.

| Parameters | Values | References |
|--|-----------------|---|
| Soil conditions (top 0.3 m) | | |
| Bulk Density (g/cm ³) | 0.069 | Miao et al. (2009, 2010); Reddy and DeLaune (2008) |
| Soil C (μg C/cm ²) | 41961.87 | Miao et al. (2009, 2010) |
| Soil N (μg N/cm ²) | 2588.87 | Miao et al. (2009, 2010) |
| Soil P (μg P/cm ²) | 58.5 | Miao et al. (2009, 2010) |
| Nutrients in surface water | | |
| NH ₄ (mg N/L) | 0.0161 | Qualls and Richardson (2003) |
| NO ₃ (mg N/L) | 0.0195 | Qualls and Richardson (2003) |
| PO ₄ (μg P/L) | 44.1 | Qualls and Richardson (2003) |
| POC (mg C/L) | 3.198 | Qualls and Richardson (2003); Miao et al. (2009, 2010) |
| PON (mg N/L) | 0.1599 | Qualls and Richardson (2003); Miao et al. (2009, 2010) |
| POP (μg P/L) | 0.78 | Qualls and Richardson (2003); Miao et al. (2009, 2010) |
| DOC (mg C/L) | 30.6270 | Qualls and Richardson (2003); Miao et al. (2009, 2010) |
| DON (mg N/L) | 1.5314 | Qualls and Richardson (2003); Miao et al. (2009, 2010) |
| DOP (μg P/L) | 7.5 | Qualls and Richardson (2003); Miao et al. (2009, 2010) |
| Nutrients in pore water | | |
| NH ₄ (mg N/L) | 0.129 | Miao et al. (2009, 2010) |
| NO ₃ (mg N/L) | 0.007 | Miao et al. (2009, 2010) |
| PO ₄ (μg P/L) | 52 | Miao et al. (2009, 2010) |
| POC (mg C/L) | 13.55 | Calculated based on surface water concentration and Fire Project observations |
| PON (mg N/L) | 0.512 | Calculated based on surface water concentration and Fire Project observations |
| POP (μg P/L) | 1.23 | Calculated based on surface water concentration and Fire Project observations |
| DOC (mg C/L) | 129.8 | Miao et al. (2009, 2010) |
| DON (mg N/L) | 4.90 | Calculated based on surface water concentration and Fire Project observations |
| DOP (μg P/L) | 12 | Calculated based on surface water concentration and Fire Project observations |
| Cattail biomass | | |
| Leaf (C, N, P) (g/m ²) | 200, 3.45, 0.2 | Miao et al. (2009, 2010) |
| Shoot Base (C, N, P) (g/m ²) | 160, 2.96, 0.5 | Miao et al. (2009, 2010) |
| Rhizome (C, N, P) (g/m ²) | 40, 0.65, 0.055 | Miao et al. (2009, 2010) |
| Root (C, N, P) (g/m ²) | 40, 1.9, 0.04 | Miao et al. (2009, 2010) |

Table 2
Major parameters for WEM in simulation of a highly P-enriched Everglades wetland.

| Parameters | Values | References |
|---|---------------|--|
| Plant (cattail) | | |
| Maximum Biomass C (g C/m ²) | 750 | Miao et al. (2009, 2010); Reddy et al. (1999) |
| Maximum Height (m) | 2.5 | Miao et al. (2009, 2010); Reddy et al. (1999) |
| Maximum LAI (m ² /m ²) | 4.0 | Miao et al. (2009, 2010); Reddy et al. (1999) |
| Mortality (g C/g C) | 0.0025 | Miao et al. (2009, 2010); Calibrated* |
| Res (Leaf, rhizome, shoot-base, root) (g C/g C) | 0.0002~0.0045 | Miao et al. (2009, 2010); Reddy et al. (1999); Calibrated* |
| Leaf C:N ratio (g C/g N) | 70 | Miao et al. (2009, 2010); Reddy et al. (1999); Calibrated* |
| Leaf C:P ratio (g C/g P) | 1000 | Miao et al. (2009, 2010); Reddy et al. (1999); Calibrated* |
| Rhizome C:N ratio (g C/g N) | 60 | Miao et al. (2009, 2010); Reddy et al. (1999); Calibrated* |
| Rhizome C:P ratio (g C/g P) | 750 | Miao et al. (2009, 2010); Reddy et al. (1999); Calibrated* |
| Shoot-Base C:N ratio (g C/g N) | 54 | Miao et al. (2009, 2010); Reddy et al. (1999); Calibrated* |
| Shoot-Base C:P ratio (g C/g P) | 350 | Miao et al. (2009, 2010); Reddy et al. (1999); Calibrated* |
| Root C:N ratio (g C/g N) | 35 | Miao et al. (2009, 2010); Reddy et al. (1999); Calibrated* |
| Root C:P ratio (g C/g P) | 1000 | Miao et al. (2009, 2010); Reddy et al. (1999); Calibrated* |
| N resorption (g N/g N) | 0.45 | Miao et al. (2009, 2010); Reddy et al. (1999); Calibrated* |
| P resorption (g P/g P) | 0.75 | Miao et al. (2009, 2010); Reddy et al. (1999); Calibrated* |
| Hydrological | | |
| PON sedimentation (g nutrient/ g nutrient) | 0.075 | Calibrated* |
| Diffusion (g nutrient/g nutrient/hour) | 0.035~0.055 | Reddy et al. (1999); Calibrated* |
| Soil | | |
| Bottom temperature (°C) | 5 | Miao et al. (2009, 2010); calibrated* |
| Maximum adsorbed NH ₄ (μg N/cm ³) | 25 | Calibrated*; Reddy et al. (1999) |
| Half-saturation coefficient of adsorbed NH ₄ (μg N/cm ³) | 5 | Calibrated*; Reddy et al. (1999) |
| Maximum adsorbed NO ₃ (μg N/cm ³) | 25 | Calibrated*; Reddy et al. (1999) |
| Half-saturation coefficient of adsorbed NO ₃ (μg N/cm ³) | 5 | Calibrated*; Reddy et al. (1999) |
| Maximum adsorbed PO ₄ (μg N/cm ³) | 2.5 | Calibrated*; Reddy et al. (1999) |
| Half-saturation coefficient of adsorbed PO ₄ (μg N/cm ³) | 0.5 | Calibrated*; Reddy et al. (1999) |
| Fire | | |
| Fire Intensity (fraction of litter burned out) | 0.9 | Miao et al. (2009, 2010); Calibrated* |
| Leaf C Fire Efficiency (gCO ₂ /g C) | 0.7 | Miao et al. (2009, 2010); Calibrated* |
| Leaf N Fire Efficiency (gNO _x /g C) | 0.55 | Miao et al. (2009, 2010); Calibrated* |
| Litter C Fire Efficiency (gCO ₂ /g C) | 0.95 | Miao et al. (2009, 2010); Calibrated* |
| Litter N Fire Efficiency (gNO _x /g C) | 0.9 | Miao et al. (2009, 2010); Calibrated* |

* Calibrated: parameters were adjusted to make the output comparable against observed data.

Table 3

Site descriptions including parameters and data used to calibrate and validate the WEM (Most of the input data and a portion of the data used for calibration are from DBHYDRO, the South Florida Water Management District’s environmental database).

| Site name | Location | Variables | Data sources |
|---|--------------------|--|--|
| Major input data | | | |
| WCA2F4 | N26.32, W80.38 | Rainfall, solar radiation, air temperature, PAR | DBHYDRO |
| WCA2E1 | N26.35, W80.35 | Reference water depth | DBHYDRO |
| Gainesville, Cedar Key, Apopka, Belle Glade | Four sites average | N and P deposition | Brezonik and Pollman, 1999 |
| Site and major parameters for model calibration | | | |
| H1 (unburned area; cattail dominated) | N26.35, W80.37 | Cattail aboveground biomass Cattail belowground biomass Cattail aboveground dead mass Cattail belowground dead mass Water depth Surface-water TP Soil TP | Miao et al. (2009, 2010) Miao et al. (2009, 2010) |
| Site and major parameters for model validation | | | |
| H2 area (burned area; cattail dominated) | N26.35, W80.35 | Cattail aboveground biomass Cattail belowground biomass Cattail aboveground dead mass Cattail belowground dead mass Water depth Surface-water TP Soil TP Soil and surface-water temperature Fire released CO ₂ Fire released NO _x | Miao et al. (2009, 2010) Miao et al. (2009, 2010) |

the simulation period. The differences between these two scenarios were regarded as the fire impacts. Due to continuous inflow and outflow, no hydrologic equilibrium existed in this system. To solve this issue we assumed that the average daily climate and inflow data for a ten year period (1998–2008) would be representative of the long term conditions in the Everglades. Therefore we used those data as the input data to forecast the system responses for 50 years. The simulation was extended to cover the period 1998–2008 to validate our assumption. The 50-year period was selected because P loading to the Everglades has occurred over the past half century (Miao and DeBusk, 1999). Because the WEM is a site-level biogeochemical model, it could not evaluate downstream effects directly. The downstream effect was addressed by running two simulations with the outflow from one simulation serving set as the inflow to the second simulation. The cell size for the simulation was set at 300 m × 300 m to be consistent with the layout of the Fire Project field experiment.

2.4. Statistical methods used to compare the model and data fit

A total of five criteria were used to evaluate the modeled results against observations. The first one is the coefficient of determination (R^2) which is calculated as the correlation between observations and predictions; higher R^2 means better model performance. The second criterion is the Theil's inequality coefficient (Theil, 1966; Blanco et al., 2007) which is calculated as:

$$U = \sqrt{\frac{\sum_{i=1}^n D_i^2}{\sum_{i=1}^n \text{Observed}_i^2}}$$

where $D_i = \text{observed}_i - \text{predicted}_i$ and n is the number of data pairs. Parameter U could be 0 or greater. $U=0$ means the perfect fit between model results and observations. Larger U value means poorer model performance (Blanco et al., 2007). The third index used is modeling efficiency (ME) (Vanclay and Skovsgaard, 1997):

$$ME = 1 - \frac{\sum D_i^2}{\sum (\text{Observed}_i - \text{Predicted}_i)^2}$$

where $ME = 1$ indicates a perfect fit, $ME = 0$ reveals that the model is no better than a simple average, and negative values indicate poor performance. The fourth index is the average absolute bias (AAB), expressed as a percentage. This method has been used in the intergovernmental panel on climate change (IPCC) report (Penner et al., 2001).

$$AAB = \sum_{i=1}^n \left(\frac{\text{Predicted}_i - \text{Observed}_i}{\text{Observed}_i} \times 100 \right)$$

The fifth criterion is the equivalence test parameters; equivalence testing is a powerful method to evaluate the comparison between observations and the predictions (Fujisaki et al., 2009). Contrasting with the traditional t -tests, the equivalence test evaluates the null hypothesis of dissimilarity. Two criteria (ϵ) were expressed relative to the sample standard deviation (25% and 50%) to represent a “strict” and “liberal” criterion, respectively, according to the guidelines in Wellek (2003). The t value was calculated as follows:

$$td = \frac{\bar{D}_i}{S_{D_i}}$$

The calculated t value was then compared with cutoff value of C , which is the α -quantile (0.05 in this study) of the non-central F distribution with degrees of freedom $\nu_1 = 1$ and $\nu_2 = n - 1$ and non-centrality parameter $\lambda = n\epsilon^2$. If the t value was lower than the cutoff value, the null hypothesis of dissimilarity was rejected (Robinson and Froese, 2004). In essence, the test is used to check whether the critical value of a two-tailed F distribution (the C parameter) are contained within the rejection region defined by the selected criteria ($-\epsilon, +\epsilon$) (Blanco et al., 2007). The power of this test was calculated using the following equation (Wellek, 2003):

$$\beta_{\alpha;n-1}(\epsilon) = 2Ft(C_{\alpha;n-1}(\epsilon)) - 1$$

where F_t is the cumulative distribution function for the non-central t -distribution (Robinson and Froese, 2004).

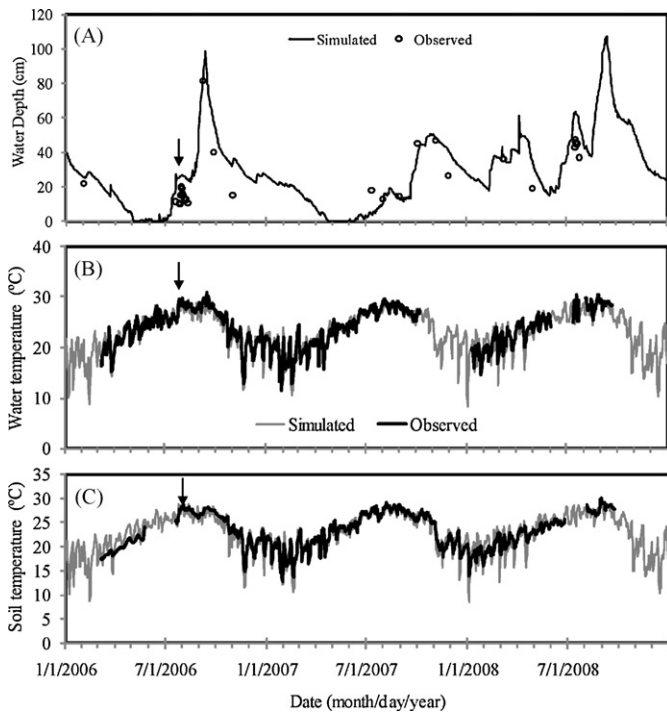


Fig. 2. Comparison of simulated (A) water depth, (B) surface-water and (C) soil temperature to observation data from the Fire Project (The arrows show the date of burn).

3. Results

3.1. Model validation

Model validation is a critical component for model development and application (Haefner, 2005; Blanco et al., 2007). In this study, the WEM was verified by comparing simulated results against field data collected 10 days prior or after the burning date (Figs. 2–4, and Table 4). For the time-series comparison, five criteria were used to evaluate the model performance in simulating water depth, water and soil temperature, TP in surface- and pore-water, and cattail biomass and dead mass (Table 5). The model performance

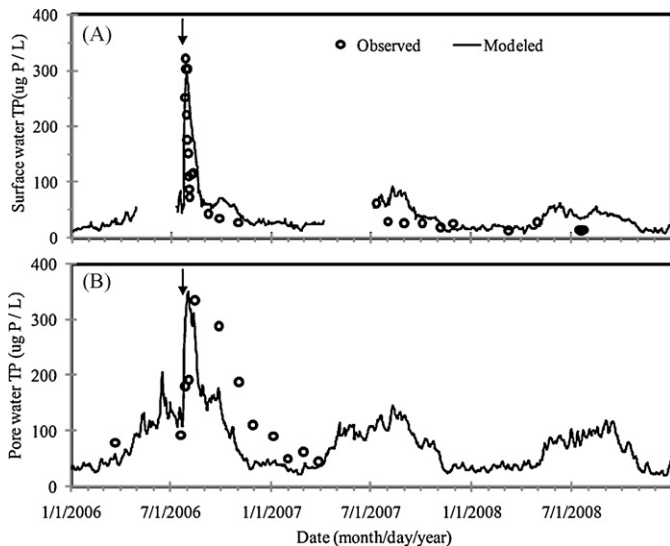


Fig. 3. Comparison of simulated (A) surface-water and (B) pore-water total phosphorus (DOP, POP, and DIP included) to observed data from the Fire Project and DBHYDRO database (my.sfwmd.gov) (The arrows show the date of burn).

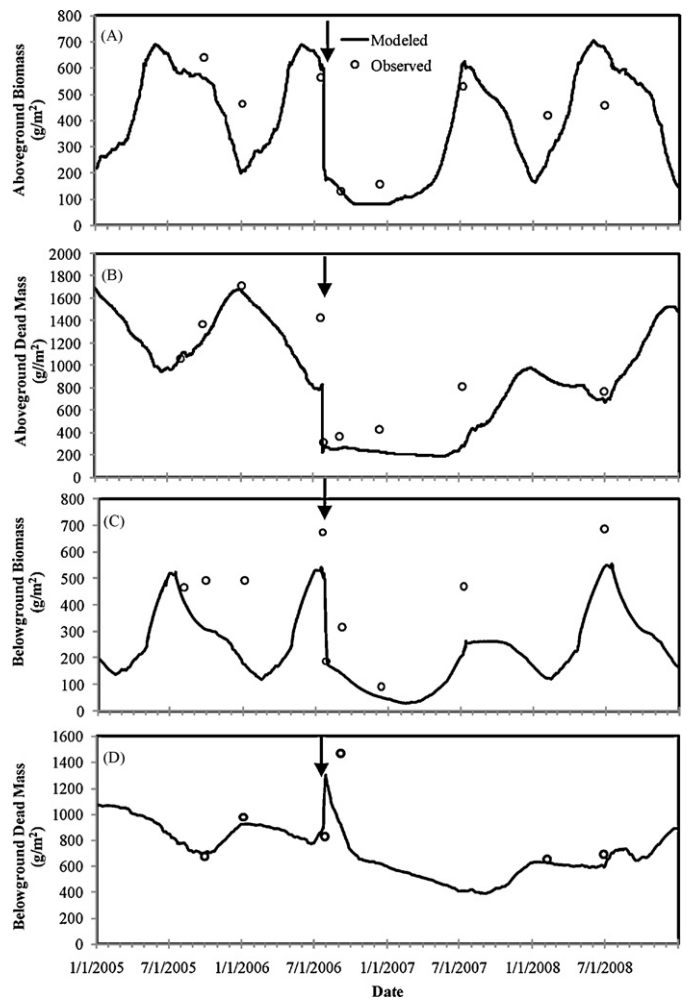


Fig. 4. Comparison of simulated cattail aboveground and belowground, biomass and dead mass and observed data from the Fire Project (A. aboveground biomass; B. belowground biomass; C. aboveground dead mass; D. belowground dead mass) (The arrows show the date of burn).

was first evaluated based on the coefficient of determination (R^2). Simulated water depths values agreed well with the field measurements from the Fire Project’s burned plot (Fig. 2); approximately 79% of the variability observed in the water depth was accounted for by the simulation ($R^2 = 0.79$). Simulated surface-water and soil temperatures also were consistent, both seasonally and quanti-

Table 4

Comparison of simulated ecosystem properties to observed data (on date of burn or less than 10 days before the burn date) from the Fire Project.

| Variables | Simulated | Observed |
|--|-----------|----------|
| Cattail aboveground biomass (g/m^2) [*] | 619.21 | 564.10 |
| Cattail aboveground dead mass (g/m^2) [*] | 1214.49 | 1432.10 |
| Cattail belowground biomass (g/m^2) [*] | 509.25 | 673.60 |
| Cattail belowground dead mass (g/m^2) [*] | 595.10 | 517.70 |
| Surface-water TP ($\mu\text{g P}/\text{L}$) ^{**} | 262.85 | 253.93 |
| Pore-water TP ($\mu\text{g P}/\text{L}$) ^{***} | 279.60 | 236.33 |
| Soil TP ($\mu\text{g P}/\text{cm}^3$) ^{****} | 95.19 | 94.88 |
| Fire released CO_2 ($\text{g C}/\text{m}^2$) | 420.86 | 548.54 |
| Fire released NO_x ($\text{g N}/\text{m}^2$) | 7.22 | 8.53 |

^{*} Simulated and observed cattail above- and below-ground biomass and dead mass are 10 days before fire.

^{**} Simulated and observed surface-water TP concentrations are 5-day post-fire average.

^{***} Simulated and observed pore-water TP concentrations are 30-day post-fire average.

^{****} Simulated and observed soil TP concentrations are 3-year (2006–2008) average.

tatively, with field measurements (Fig. 2); approximately 90% of the variability in the surface-water temperature was accounted for by the simulations ($R^2 = 0.90$), and approximately 83% of the variability in soil temperature was explained by the simulations ($R^2 = 0.83$). The WEM simulation results were also consistent with the observed cattail dynamics, including aboveground biomass and dead mass, belowground biomass and dead mass, TP in surface-water, pore-water, and soil, and fire released C and NO_x (Table 4). The simulations explained 69% of the variability in surface-water TP ($R^2 = 0.69$), and 53% of the variability in pore-water TP ($R^2 = 0.53$) (Fig. 3A and B). Comparison of seasonal pattern of WEM simulated cattail biomass and dead mass revealed the WEM's ability to accurately simulate post-fire cattail growth. The WEM simulation captured approximately 63%, 81%, 62%, and 24% of the variability in observed cattail aboveground biomass, aboveground dead mass, belowground biomass, and belowground dead mass, respectively, over three years (Fig. 4A–D).

We also evaluated the model performance by using the Theil's index, modeling efficiency, average absolute bias, and equivalence test. The calculated Theil's index for the comparisons of modeled and observed variables indicated good performance of the WEM model in simulating all variables because of the relatively low U index (Table 5). The calculated modeling efficiencies showed that the WEM model did well in simulating water depth, water and soil temperatures, TP concentration in surface- and pore-water, aboveground biomass and dead mass, although it did not do so well in simulating belowground biomass and dead mass (Table 5). The calculated average absolute biases showed small biases in simulating water and soil temperatures, pore-water TP, and cattail biomass, while relatively high biases in simulating water depth and surface water TP (Table 5). The equivalence test showed that the WEM performed well in simulating water and soil temperatures, while it did not do so well in simulating water depth, surface- and pore-water TP, and cattail biomass and dead mass (Table 5). The null hypothesis of dissimilarity were not rejected for the comparisons of modeled and observed variables of water depth, surface- and pore-water TP, cattail biomass; while the t values for all variables were not far from the cutoff value, indicating the relatively good performance of the WEM in simulating all variables.

3.2. Sensitivity analysis

Sensitivity analysis is a powerful tool to reveal how model uncertainty can be apportioned to the variability in parameters, input data, or other factors (Haefner, 2005). In this study, initial conditions, major input data, and parameters were selected as given factors for this analysis. Model behavior in response to various factors was evaluated based on changes in vegetation components and the TP content in plants, soil, and surface-water, a few days before the date of the burn. The model responses to the prescribed fire were represented as the recovery percentage, comparing to the unburned scenario, for the plant tissue 365 days after the fire, for the surface-water TP 5 days after the fire, for the pore-water TP 30 days after the fire, and for the average soil TP 3 years post-fire. Two groups of factors were included in the sensitivity analysis. The first group including reference water depth and air temperature were set to changes at a rate of absolute value; the second group including fire intensity, mortality, rainfall, photosynthetically active radiation (PAR), and solar radiation were set to changes at a rate of percent change. Owing to the 50-year pre-simulation, the changes in initial conditions have no impacts on cattail tissues, surface- and pore-water TP, and soil TP. Plant mortality exerted significant impacts on the P dynamics in the system including TP in cattail tissue, surface- and pore water, and soil. The N resorption slightly changed the cattail biomass and dead mass on the burn date, while the P resorption had no impact on these

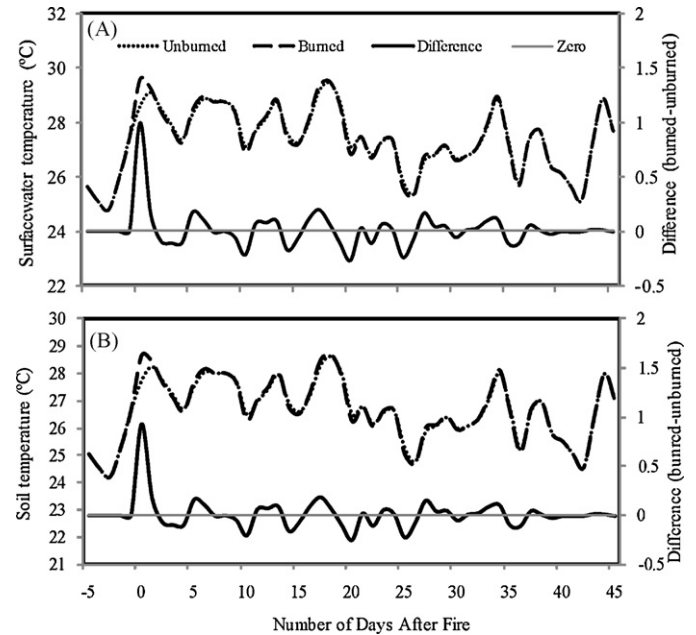


Fig. 5. Simulated post-fire dynamics of (A) surface water and (B) soil temperature. (All values are daily averages).

components. These distinctive responses implied that the nutrient enriched area in the Everglades is close to being P-saturated (Richardson and Qian, 1999), but still slightly responsive to N. Although the changes in diffusion, and decomposition of PON and DON did lead to a small shift of TP in cattail biomass, surface-water, pore-water and soil TP; they caused no changes in cattail aboveground, and belowground biomass and dead mass. This implied that the small changes in soil and surface-water had no substantial influence on cattail growth, which further confirmed that the cattail ecosystem in the P-enriched area of the Everglades is close to being P-saturated.

Almost all the input data influenced the recovery time for cattail aboveground biomass. Recovery percentage for aboveground dead mass, belowground biomass and dead mass were also influenced by most of the input data and major parameters (Table 6). Water depth changed the cattail biomass recovery time and changes in ecosystem P pools; lower water depth on the date of burn increased the biomass and dead mass consumed in fire; and air temperature exerts significant impacts on cattail biomass recovery time and P pool size in the ecosystem (Table 6). Fire intensity affected the recovery of cattail biomass recovery to unburned levels, more intensive fires lengthened the recovery time for aboveground dead mass to unburned condition, while shortening the recovery time for aboveground biomass, belowground biomass and dead mass (Table 6). This may be because more intense fires consume more original cattail plant, and more new ramets will be generated from the nutrient storage pool (mainly rhizome and shootbase) (Miao et al., 2009); these new ramets usually grow faster than the original plant ramets (Miao et al., 2009). This also suggested that more attention should be paid to the fire intensity effects on cattail dynamics. Plant mortality was another important parameter which may significantly influence the cattail growth (Table 6). Changes in PAR and rainfall did not cause significant changes in cattail biomass; this indicates that the system was saturated for PAR and rainfall. In summary, the sensitivity analysis revealed that water depth and air temperature were the two most important factors affecting the recovery time of aboveground biomass, aboveground dead mass, belowground biomass, and dead mass, back to unburned levels. This suggested that the water depth and air temperature are two

Table 5
Statistical comparison of the overall fit of model outputs against field data (see footnotes).

| Statistic | Water depth | Water temperature | Soil temperature | Surface water TP | Pore water TP | AGB | AGDM | BGB | BGDM |
|---------------------------|-------------|-------------------|------------------|------------------|---------------|--------|--------|-------|-------|
| R ² | 0.79 | 0.90 | 0.83 | 0.69 | 0.53 | 0.63 | 0.81 | 0.62 | 0.24 |
| U | 0.42 | 0.05 | 0.07 | 0.53 | 0.47 | 0.31 | 0.28 | 0.38 | 0.28 |
| ME | 0.50 | 0.90 | 0.82 | 0.57 | 0.50 | 0.62 | 0.64 | -0.26 | -0.77 |
| Average absolute bias (%) | 53.72 | 0.63 | -0.73 | 80.38 | -18.00 | -10.02 | -24.85 | -28.3 | -1.96 |
| t _d | 6.41 | 2.37 | 3.99 | 3.22 | 0.74 | 0.53 | 2.58 | 3.26 | 0.47 |
| C (ε = 25%) | 0.027 | 28.63 | 31.03 | 0.02 | 0.01 | 0.007 | 0.007 | 0.007 | 0.006 |
| C (ε = 50%) | 1.28 | 151.27 | 162.25 | 0.99 | 0.08 | 0.03 | 0.04 | 0.04 | 0.02 |
| Diss (ε = 25%) | NR | R | R | NR | NR | NR | NR | NR | NR |
| Diss (ε = 50%) | NR | R | R | NR | NR | NR | NR | NR | NR |
| B (ε = 25%) | 0.94 | 1 | 1 | 0.92 | 0.54 | 0.38 | 0.42 | 0.42 | 0.29 |
| B (ε = 50%) | 1 | 1 | 1 | 1 | 0.997 | 0.95 | 0.97 | 0.97 | 0.86 |
| N | 31 | 786 | 836 | 28 | 12 | 8 | 9 | 9 | 6 |

Note: R², coefficient of determination; U, Theil's coefficient; ME, modeling efficiency; t_d: equivalence t value; C, equivalence cutoff; ε, criteria of 25% and 50%; Diss, hypothesis of dissimilarity (NR, not rejected; R, rejected); β, power of the equivalence test (see text for details); AGB: Aboveground Biomass; BGB: Belowground Biomass; ADM: Aboveground Dead Mass; BDM: Belowground Dead Mass).

important factors that should be considered in future studies of fire management in the Everglades.

3.3. Post-fire dynamics of surface-water and soil temperature

Simulated water and soil temperature were altered by the prescribed fire. Fire increased water temperature up to 1.0 °C (Fig. 5a), and soil temperature up to 0.93 °C (Fig. 5b). One week after the burn, the water temperature started to fluctuate, closely following the fluctuation of air temperature, suggesting that the open canopy caused by the fire was the more plausible reason for water temperature fluctuations (Fig. 5a). The fire effects diminished 4–5 weeks after the fire. The changing pattern implied that the fire's direct heating effect was strong on the day of the burn and in the following two days; however the fire's indirect effect became predominant three days after fire and lasted for approximately one month. Post-fire changes in soil temperature were similar to those of surface-water temperature (Fig. 5b), confirming that soil temperature was controlled by water temperature.

3.4. Post-fire dynamics of cattail biomass

When fire occurred, the aboveground biomass was at its peak, the aboveground dead mass was increasing, belowground biomass was decreasing, and belowground dead mass had started to decrease; fires changed these trends. The simulations showed that the prescribed fire reduced the cattail aboveground biomass and dead mass, and belowground biomass by 62.11%, 72.05%, and 14.01%, respectively, and increased belowground dead mass by 12.15% (Fig. 6). Although cattail's aboveground biomass reached the unburned level one year after burn, the belowground biomass recovered to unburned level one and half years after the fire, and the aboveground and belowground dead mass did not completely reach unburned level even two years after fires.

3.5. Post-fire dynamics of P in surface- and pore-water

The simulation showed that fire altered the ecosystem directly by changing the plant biomass and water temperature, and indirectly altering P dynamics in the water. The simulations showed that the prescribed fire created a P pulse in surface water (Fig. 7a). This was because the fire-generated ash P returned to the system and either directly or indirectly increased the concentrations of POP, DOP, and DIP. The magnitude of the surface-water TP increase caused by the fire was up to approximately 215 μg P/L on 4 days post-fire, which was consistent with the observations from the Fire Project. The fire effects on surface-water TP lasted five weeks (approximately 35 days), after elevated P concentrations declined

until no difference between the burned and unburned plots was detectable.

The prescribed fire not only changed the surface-water TP, but also changed the pore-water TP. A pulse in pore-water TP, with

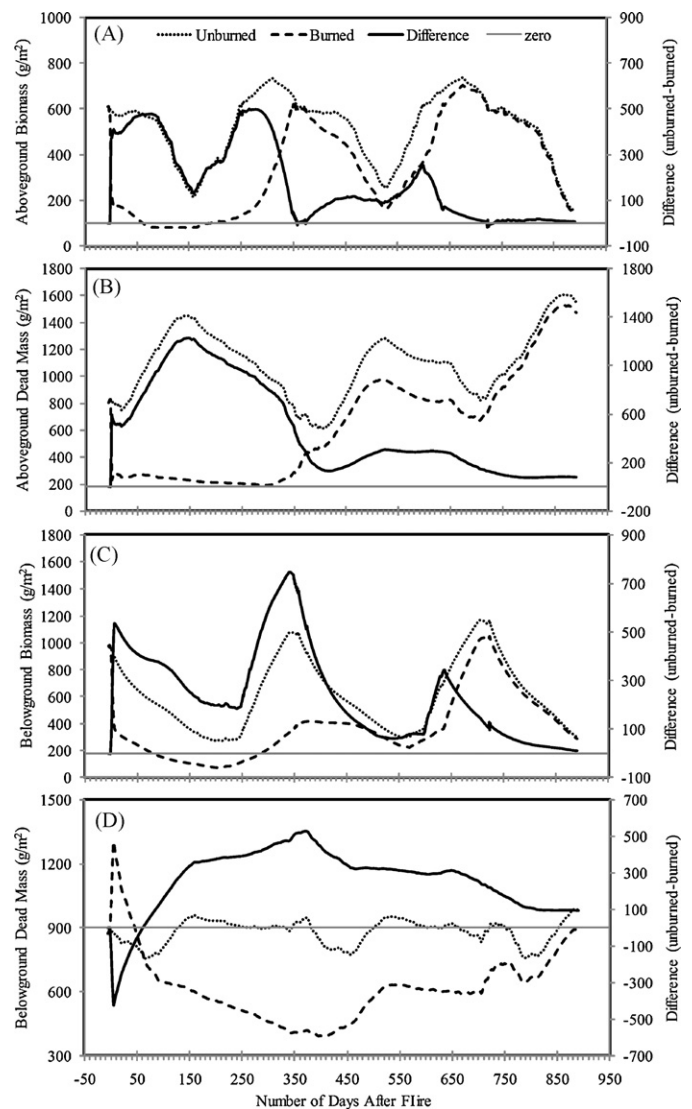


Fig. 6. Simulated post-fire dynamics of cattail aboveground and belowground biomass and dead mass (A. aboveground biomass; B. belowground biomass; C. aboveground dead mass; D. belowground dead mass).

Table 6
Sensitivity analysis of the WEM based on model behavior in response to various initial states and parameters represented by the biomass of vegetation components, surface-water TP, pore-water TP, and soil TP on the date of burn. The model responses to the prescribed fire are represented by recovery percentages for plant tissues 365 days after fire, surface-water TP 5 days after fire, pore-water TP 30 days after fire, and soil TP 365 days after fire, respectively, comparing to unburned scenario; AGB: Aboveground Biomass; BGB: Belowground Biomass; ADM: Aboveground Dead Mass; BDM: Belowground Dead Mass).

| Input Parameters | Changes | Δ AGB (%) | | Δ AGDM (%) | | Δ BGB (%) | | Δ BGDM (%) | | Δ Surface-water TP (%) | | Δ Pore-water TP (%) | | Δ Soil TP (%) | |
|------------------------------------|---------|------------------|--------|-------------------|--------|------------------|--------|-------------------|--------|-------------------------------|-------|----------------------------|--------|----------------------|--------|
| | | Mag. | Rec. | Mag. | Rec. | Mag. | Rec. | Mag. | Rec. | Mag. | Rec. | Mag. | Rec. | Mag. | Rec. |
| Initial conditions | | | | | | | | | | | | | | | |
| Initial state (plant, soil, water) | –10% | 0.00 | 0.00 | 0.00 | 0.00 | 0.00 | 0.00 | 0.00 | 0.00 | 0.00 | 0.00 | 0.00 | 0.00 | 0.00 | 0.00 |
| | +10% | 0.00 | 0.00 | 0.00 | 0.00 | 0.00 | 0.00 | 0.00 | 0.00 | 0.00 | 0.00 | 0.00 | 0.00 | 0.00 | 0.00 |
| Major parameters | | | | | | | | | | | | | | | |
| Fire intensity | –10% | 0.00 | 0.65 | 0.00 | 4.03 | 0.00 | 4.73 | 0.00 | 5.7 | 0.00 | –7.40 | 0.00 | –3.55 | 0.00 | –7.66 |
| | +10% | 0.00 | –1.12 | 0.00 | –3.29 | 0.00 | –0.99 | 0.00 | –2.92 | 0.00 | 7.43 | 0.00 | 4.22 | 0.00 | 5.49 |
| Plant mortality | –20% | 0.29 | 2.42 | 0.79 | 6.79 | 14.84 | 24.44 | 6.31 | 19.33 | –3.67 | 8.22 | –3.91 | 11.69 | –3.79 | –5.31 |
| | +20% | –69.1 | –4.37 | –77.41 | 66.41 | –71.6 | 82.59 | –76.68 | 104.24 | –70.39 | 53.92 | –73.82 | –53.07 | –2.1 | –83.96 |
| N resorption | –10% | 1.16 | –1.3 | –0.48 | –0.79 | –2.24 | –0.73 | –1.54 | –0.86 | 1.07 | –0.21 | –0.16 | –0.76 | –0.08 | 0.76 |
| | +10% | 0.91 | 3.42 | 0.80 | –0.59 | 0.32 | –4.19 | 0.66 | –0.68 | –1.41 | 0.35 | –0.28 | –0.30 | 0.07 | 0.07 |
| P resorption | –10% | 0.00 | 0.00 | 0.00 | 0.00 | 0.00 | 0.00 | 0.00 | 0.00 | 3.28 | –1.39 | 0.97 | –0.37 | 0.01 | 1.42 |
| | +10% | 0.00 | 0.00 | 0.00 | 0.00 | 0.00 | 0.00 | 0.00 | 0.00 | –3.32 | 1.78 | –0.96 | 0.44 | –0.01 | –1.74 |
| Diffusion | –10% | 0.00 | 0.00 | 0.00 | 0.00 | 0.00 | 0.00 | 0.00 | 0.00 | –0.36 | 2.09 | 5.71 | 1.23 | 0.01 | –0.09 |
| | +10% | 0.00 | 0.00 | 0.00 | 0.00 | 0.00 | 0.00 | 0.00 | 0.00 | 0.27 | –1.74 | –4.7 | –1.27 | –0.01 | 0.01 |
| PON decomposition | –10% | 0.00 | 0.00 | 0.00 | 0.00 | 0.00 | 0.00 | 0.00 | 0.00 | 2.31 | –0.12 | 1.62 | 4.88 | 0.00 | –0.04 |
| | +10% | 0.00 | 0.00 | 0.00 | 0.00 | 0.00 | 0.00 | 0.00 | 0.00 | –1.83 | –0.14 | –1.25 | –3.85 | 0.00 | 0.08 |
| DON decomposition | –10% | 0.00 | 0.00 | 0.00 | 0.00 | 0.00 | 0.00 | 0.00 | 0.00 | 3.2 | –2.78 | 1.82 | –1.67 | 0.01 | –0.06 |
| | +10% | 0.00 | 0.00 | 0.00 | 0.00 | 0.00 | 0.00 | 0.00 | 0.00 | –2.56 | 2.43 | –1.41 | 1.40 | –0.01 | –0.01 |
| Driving data | | | | | | | | | | | | | | | |
| Reference water depth | –0.25m | –0.41 | –2.19 | –14.21 | 0.05 | –1.18 | –1.74 | –2.83 | –5.04 | 22.34 | 38.40 | –3.25 | 150.53 | –24.64 | 27.14 |
| | +0.25m | 1.56 | –0.44 | 41.34 | –5.51 | –2.79 | –0.06 | –2.56 | 7.38 | –21.13 | –7.78 | 0.52 | –1.38 | 18 | –19.60 |
| Rainfall | –10% | 0.00 | 0.00 | –0.41 | 0.16 | –0.03 | –0.03 | –0.61 | 0.19 | 1.77 | 0.26 | 0.44 | 1.13 | –0.31 | 0.08 |
| | +10% | 0.00 | 0.00 | 0.41 | –0.06 | 0.09 | 0.14 | 1.53 | 0.67 | –1.74 | –0.96 | 0.1 | –1.43 | 0.26 | 0.13 |
| Air temperature | –2.5 °C | –76.19 | –4.1 | –72.63 | 46.34 | –76.47 | 82.55 | –66.87 | 121.75 | –72.27 | 88.03 | –74.5 | –52.37 | –26.65 | –74.71 |
| | +2.5 °C | –35.14 | –7.18 | –80.24 | 68.96 | –55.76 | 73.48 | –83.69 | 80.83 | –66.45 | 7.67 | –73.6 | –32.59 | –30.18 | –74.46 |
| PAR | –10% | –0.17 | –27.01 | –0.78 | –22.54 | –1.02 | –15.58 | –1.96 | –7.78 | –2.23 | –0.62 | –2.06 | –3.69 | –3.1 | 0.79 |
| | +10% | 0.19 | –1.54 | 0.77 | 5.54 | 0.4 | 20.01 | 1.22 | 12.62 | 1.69 | 0.68 | 1.54 | 4.96 | 2.13 | –0.93 |

The parameters are changed from the calibrated value in Table 2, either by 10% or by a specified quantity. The changes of climate drivers for each day are based on daily climate data.

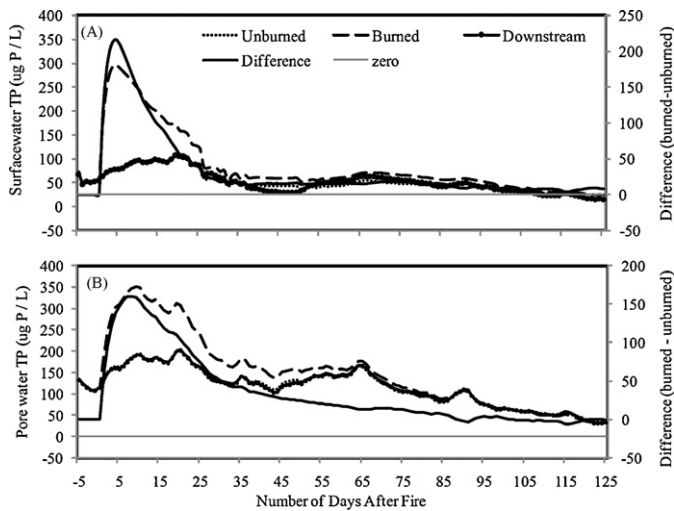


Fig. 7. A) Simulated post-fire dynamics of (A) surface-water and (B) pore-water total phosphorus (TIP + DOP + POP) in the burned plot and the 300m downstream plot.

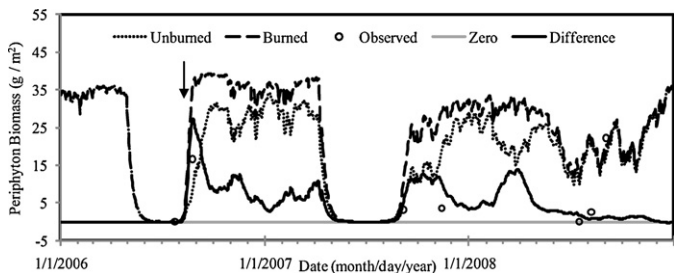


Fig. 8. Simulated post-fire dynamics of periphyton biomass (The arrow shows the date of burn).

a small magnitude, a slower increase rate and longer duration than the surface-water P pulse (Fig. 7b), was observed. The instant increase in surface-water P and delayed increase in pore-water TP suggested a fast return of ash P to the surface-water P pools. Fire caused an increase of up to 159 µg P/L in the pore-water TP almost 10 days after fire, and then the surface-water TP started to decrease pore-water TP gradually increased, which suggested that pore-water acted as a buffer sink for surface-water P. After this, plant biomass start to recover by taking up P, and portions of P started to accumulate in the SOM. The dynamics of downstream surface- and pore-water TP were similar to those in the unburned scenario (Fig. 7).

3.6. Downstream effects of the prescribed fire

One of the characteristic features of wetland ecosystems is the nutrient transport associated with inflow and outflow (Mitsch and Gosselink, 2007; Reddy and DeLaune, 2008). The fire-induced P alterations increased the P concentration in outflow from the burned plot, which have affected downstream ecosystem. The fire-induced change in downstream ecosystem was defined as downstream effects in this study. It has been evaluated by using two simulations of which outflow from one simulation was treated as inflow for the second simulation. Changes in downstream surface-water and pore-water TP concentration were used as the indicator for checking the P change caused by the upstream fire. Fig. 7A and B show the downstream P change in surface- and pore-water after the prescribed fire. There was only a small difference in surface- and pore-water TP concentration between the downstream and the unburned scenarios.

3.7. Post-fire dynamics of periphyton

The prescribed fire also stimulated periphyton biomass increase (Fig. 8), which may have been caused by increased light through the open canopy created by the burn. This was supported by previous studies, in which periphyton was reported as being light-limited (Buzzelli et al., 2000; Inglett et al., 2004; Reddy and DeLaune, 2008). One year after fire, in line with the recovered cattail biomass, periphyton biomass decreased to its unburned level (Fig. 8). The changes in periphyton biomass suggested that periphyton may also be used as an indicator for cattail growth and recovery. Due to the limited data points ($N=6$), we did not statistically compare the simulated and observed results; however, Fig. 8 did show the consistency between simulated and observed periphyton biomass along the study period (Fig. 8).

4. Discussion

4.1. Ecological and statistical evaluation of model performance

The WEM model is reasonably good in simulating water depth, water and soil temperature, TP in surface- and pore-water, cattail growth (Table 5). The simulated seasonal variations of water depth, temperature, water TP and cattail growth are consistent with field observations both quantitatively and in seasonal pattern; this suggests that the WEM is able to represent major variables in the P-enriched wetlands in the Everglades in response to fires. The statistical evaluation of the modeled results compared to the field observations suggests the capacity of WEM in effectively simulating the system's responses to fire.

The evaluation of model performance should also consider the potential biases from field measurements. As Blance et al. stated (2007), when validating complex models with multiple output variables, it is necessary to carefully consider the level of confidence in field-measured variables and associated interpretations or summaries. The challenge in sampling plant in wetland has long been treated as one of the major uncertainty sources in wetland studies due to either the difficulty of sampling plant organs, or the high spatial heterogeneity of plant and soil properties in wetlands (Mitsch and Gosselink, 2007; Reddy and DeLaune, 2008). So the errors in field sampling might be one of the major reasons for biases in model validations.

4.2. Fire effects on ecosystem properties

The immediate increases in water and soil temperatures after fires may have been due to the following factors: (1) direct heating of the water by the fire, and/or (2) indirect effects caused by the fire-induced canopy gap, which allowed more incoming solar radiation (Gu et al., 2008; Neary et al., 2005). Heat produced during the combustion of aboveground fuels could be transferred to the water surface and downward through the soil by several heat transfer processes such as radiation, convection, conduction, vaporization, and condensation (Neary et al., 2005). These processes directly and/or indirectly caused the changes in water and soil temperature observed in this study.

The post-fire prompt recovery of aboveground biomass and the slow recovery of dead mass were consistent with the field experiment in which the aboveground biomass came back to the unburned level one year after the burn, but the accumulated aboveground dead mass did not support a second burn until two years after the first burn, this has been observed in our field experiments (Miao et al., 2009). The slower recovery of aboveground dead mass compared to aboveground biomass may be one of the natural plant strategies for fire stress in terms of the long term fire

disturbances in Everglades because lower aboveground dead mass recovery decreases the chance of future burning, hence it protects cattail from fire stress (Urban et al., 1993; Wu et al., 1993).

The longer-recovery of surface water TP as simulated (approximately 35 days) was slightly different from the observed recovery period of 10 days in the field experiment (Miao et al., 2010), which probably reflected flushing from a heavy rainfall four days after the field burn that was not considered in our simulation. The reduction of pore-water TP may have been due to the equilibrium exchange between pore-water dissolved P and soil adsorbed P (Wang et al., 2007). There was only a small difference in surface- and pore-water TP concentration between the downstream and the unburned scenarios, indicating that the downstream effect was negligible 300 m downstream from the prescribed fire.

4.3. Improvements needed

This study evaluated the post-fire P dynamic in water and the associated cattail recovery in the P-enriched area in the Everglades by using a newly-developed wetland ecosystem model. Several aspects should be improved in the subsequent research. First, lack of field data in validating model might lead to uncertainty in the simulation; so more and accurate field data will improve the model behavior. Second, inclusion of N fixation in the system may improve the accuracy of model prediction of fire effects on cattail growth. Although the natural N fixation is far smaller comparing to N loading from upstream inflow (Reddy and DeLaune, 2008), the N fixation might exert effects on ecosystem dynamics in the system because the P-enriched area in the Everglades is limited by N (Reddy and DeLaune, 2008). Third, environmental factors influencing ash diffusion and fire severity, such as wind velocity and direction, and humidity, might improve the model's ability in simulating fire effects; for example the exclusion of flushing effects of precipitation has led to more than 20 days difference in recovery of surface-water TP. Fourth, exclusion of plant competition might overestimate or underestimate the cattail response to fires, which should be one of the focuses in the following efforts.

5. Conclusions

In this study, we developed and applied a wetland ecosystem model WEM to evaluate the ecosystem responses to a prescribed fire in the highly P-enriched wetland in WCA-2A. The robustness of the WEM was demonstrated by comparing the model outputs with field measurements. Agreeing with the filed studies, our key conclusions were:

1. The impacts of a single fire on cattail biomass lasted approximately one to one and half years.
2. The fire impacts on cattail dead mass may last more than two years.
3. Nutrients in water responded immediately to the fire and the effects lasted approximately one month.
4. Pore-water nutrient dynamics were altered by the prescribed fire, and the effect lasted approximately four months. However, the prescribed fire did not significantly alter the soil organic matter. The additional P in surface-water was ultimately accumulated in soil organic matter.
5. Prescribed fire had a minimal downstream effect; the distance that was impacted by prescribed fire was less than 300 m, when the size of the plot fire was 300 m × 300 m.
6. The responses of the highly P-enriched wetland to different factors varied significantly. Air temperature and water depth were the two most important driving factors controlling the ecosystem responses to prescribed fire.

We concluded from these simulations that a single prescribed fire significantly altered cattail growth and P dynamics in surface- and pore-water TP. However, further studies are needed to determine the long-term effects and multiple-fire effects in the Everglades wetland that are the ultimate goals of the Fire Project. Sensitivity analysis identified air temperature and water depth as two important factors for fire management in the Everglades' wetlands. Future studies should therefore focus more on the effects of different hydrological conditions and air temperatures on the fire effects on Everglades wetland by further application of this model.

Acknowledgements

We thank the South Florida Water Management District for financial support, and Auburn University for facility support. We also thank all the other members from Ecosystem Dynamics and Global Ecology Laboratory (EDGE) at Auburn University for their suggestions on model development and application. We appreciate Lili Carpenter, Cassandra Thomas, Binhe Gu, Christopher Edelstein, Susan Carstenn, Jason Field, Tracey Piccone, Mike Chimney, Fred Sklar, and Martha Nungesser, for reviewing the manuscript, and Grame Lockaby, for providing helpful suggestions in the early stage of this work.

References

- Abtew, W., 2005. Evapotranspiration in the Everglades: comparison of Bowen Ratio Measurements and Model Estimations. ASAE paper No.052188. St. Joseph, Mich: ASAE.
- Blanco, J.A., Seely, B., Welham, C., Kimmins, J.P., Seebacher, T.M., 2007. Testing the performance of a forest ecosystem model (FORECAST) against 29 years of field data in a *Pseudotsuga menziesii* plantation. *Can. J. Forest. Res.* 37, 1808–1820.
- Bonan, G.B., 1996. A land surface model (LSM ver. 1.0) for ecological, hydrological, and atmospheric studies: Technical description and user's guide. NCAR Tech. Note 417 + STR, 150 pp [Available from NCAR, P.O. Box 3000, Boulder, CO 80307].
- Brezonik, P.L., Pollman, C.D., 1999. Phosphorus chemistry and cycling in Florida Lakes: Global issues and local perspectives. In: Reddy, et al. (Eds.), *Phosphorus Biogeochemistry in Subtropical Ecosystems*. CRC Press, Boca Raton, FL, USA, pp. 69–110.
- Buzzelli, C.P., Childers, D.L., Dong, Q., Jones, R., 2000. Simulation of periphyton phosphorus dynamics in Everglades National Park. *Ecol. Model.* 134, 103–115.
- Burns and McDonnell, Inc. 2003. Everglades Protection Area Tributary Basins Long Term Plan for achieving water quality goals. Final Report. South Florida Water Management District, West Palm Beach, Florida, USA.
- Chen, R.H., Twilley, R.R., 1999. A simulation model of organic matter and nutrient accumulation in mangrove wetland soils. *Biogeochemistry* 44, 93–118.
- Collatz, G.J., Ball, J.T., Grivet, C., Berry, J.A., 1991. Physiological and environmental regulation of stomatal conductance, photosynthesis and transpiration: a model that includes a laminar boundary layer. *Agr. Forest. Meteorol.* 54, 107–136.
- Davis, S.M., 1994. Phosphorus inputs and vegetation sensitivity in the Everglades. In: Davis, S.M., Ogden, J.C. (Eds.), *Everglades: The Ecosystem and Its Restoration*. St. Lucie Press, Delray Beach, FL, USA, pp. 357–378.
- DeBusk, W.F., Newman, S., Reddy, K.R., 2001. Spatio-temporal patterns of soil phosphorus enrichment in Everglades Water Conservation Area 2A. *J. Environ. Qual.* 30, 1438–1446.
- Farquhar, G.D., Caemmerer, S., Berry, J.A., 1980. A biochemical model of photosynthetic CO₂ assimilation in leaves of C3 species. *Planta* 149, 78–90.
- Fitz, H.C., Triple, B., 2006. Documentation of the Everglades Landscape Model: ELMv2. 5 Overview version of full report. South Florida Water Management District, West Palm Beach, FL, USA.
- Finlayson, C.M., Rea, N., 1999. Reasons for the loss and degradation of Australian wetlands. *Wetl. Ecol. Manag.* 7, 1–11.
- Fujisaki, I., Pearlstine, L.G., Mazzotti, F.J., 2009. Validation of daily surface water depth model of the Greater Everglades based on real-time stage monitoring and aerial ground elevation survey. *Wetl. Ecol. Manag.*, doi:10.1007/s11273-009-9144-8 (Online first version).
- Granberg, G., Grip, H., Lofvenius, M.O., Sundh, I., Svensson, B.H., Nilsson, M., 1999. A simple model for simulation of water content, soil frost, and soil temperature in boreal mixed mires. *Water Resour. Res.* 35 (12), 3771–3782.
- Gu, B., Miao, S.L., Edelstein, C., Dreschel, T., 2008. Effects of a prescribed fire on dissolved inorganic carbon dynamics in a nutrient-enriched Everglades wetland. *Fundament. Appl. Limnol.* 171 (4), 263–272.
- Haefner, J.W., 2005. *Modeling Biological Systems: Principles and Applications*. Springer, New York, NY, USA.
- Inglett, P.W., Reddy, K.R., McCormick, P.V., 2004. Periphyton chemistry and nitrogenase activity in a northern Everglades ecosystem. *Biogeochemistry* 67, 213–233.
- Li, S.W., Lissner, J., Mendelssohn, I.A., Brix, H., Lorenzen, B., McKee, K.L., Miao, S.L., 2009. Nutrient and growth responses of cattail (*Typha domingensis*)

- sis) to redox intensity and phosphate availability. *Ann. Bot-London* 1-10, Doi:10.1093/aob/mcp213.
- Miao, S.L., Carstenn, S., Thomas, C., Edelstein, C., Sindhoj, E., Gu, B., 2009. Integrating multiple spatial controls and temporal sampling schemes to explore short- and long-term ecosystem response to fire in an Everglades wetland. In: Miao, S.L., Carstenn, S., Nungesser, M. (Eds.), *Real World Ecology: Large-scale and Long-term Case Studies and Methods*. Springer, New York, NY, USA, pp. 73–110.
- Miao, S.L., Edelstein, C., Carstenn, S., Gu, B., 2010. Immediate ecological impacts of a prescribed fire on a cattail-dominated wetland in Florida Everglades. *Fundam. Appl. Limnol.*, in press.
- Miao, S.L., Carstenn, S., 2005. Assessing long-term ecological effects of fire and natural recovery in a phosphorus enriched Everglades wetland: cattail expansion, phosphorus biogeochemistry, and native vegetation recovery. In: *Options for Accelerating Recovery of Phosphorus Impacted Areas of the Florida Everglades Research Plan*. South Florida Water Management District, West Palm Beach, FL, USA.
- Miao, S.L., DeBusk, W.F., 1999. Effects of phosphorus enrichment on structure and function of sawgrass and cattail communities in the Everglades. In: Reddy, K.R., O'Connor, G.A., Schelske, C.L. (Eds.), *Phosphorus Biogeochemistry in Sub-Tropical Ecosystems*. Lewis Publishers, Boca Raton, FL, USA, pp. 275–299.
- Miao, S.L., Sklar, F., 1998. Biomass and nutrient allocation of sawgrass and cattail along a nutrient gradient in the Florida Everglades. *Wetl. Ecol. Manag.* 5, 245–263.
- Mitsch, W.J., Gosselink, J.G., 2007. *Wetlands*, 4th ed. John Wiley and Sons, Inc, Hoboken, NJ, USA.
- Moser, M., Prentice, C., Frazier, S., 1996. A global overview of wetland loss and degradation. In: 6th Meeting of the Conference of the Contracting Parties in Brisbane, Australia, March 1996.
- Neary, D.G., Ryan, K.C., DeBano, L.F., 2005. Wildland fire in ecosystems: effects of fire on soils and water. *Gen. Tech. Re, RMRS-GTR-42-vol.*, 4.
- Penner, J.E., Andreae, M., Annegarn, H., Barrie, L., Feichter, J., Hegg, D., Jayaraman, A., Leaitch, R., Murphy, D., Nganga, J., Pitari, G., et al., 2001. Aerosols, their direct and indirect effects. In: Houghton, J.T., Ding, Y., Griggs, D.J., Noguera, M., van der Linden, P.J., Dai, X., Maskell, D., Johnson, C.A. (Eds.), *Climate change 2001: The scientific basis*. The Cambridge University Press, Cambridge, UK.
- Ponzio, K.J., Miller, S.J., Lee, M.A., 2004. Long-term effects of prescribed fire on *Cladium jamaicense* and *Typha domingensis* Pers. densities. *Wetl. Ecol. Manag.* 12, 123–133.
- Qualls, R.G., Richardson, C.J., 2003. Factors controlling concentration, export, and decomposition of dissolved organic nutrients in the Everglades of Florida. *Biogeochemistry* 2, 197–229.
- Raich, J.W., Rastetter, E.B., Melillo, J.M., Kicklighter, D.W., Stuedler, P.A., Peterson, B.J., Grace, A.L., Moore III, B., Vorosmarty, C.J., 1991. Potential net primary productivity in South America: Application of a global model. *Ecol. Appl.* 1, 399–429.
- Reddy, K.R., O'Connor, G.A., Schelske, C.L., 1999. *Phosphorus Biogeochemistry in Subtropical Ecosystems*. Lewis Publishers, New York, NY, USA.
- Reddy, K.R., DeLaune, R.D., 2008. *Biogeochemistry of Wetlands: Science and Applications*. CRC Press, New York, NY, USA.
- Richardson, C.J., Qian, S., Craft, C.B., Qualls, R.G., 1996. Predictive models for phosphorus retention in wetlands. *Wetl. Ecol. Manag.* 4 (3), 159–175.
- Richardson, C.J., Qian, S.S., 1999. Long-term phosphorus assimilative capacity in freshwater wetlands: a new paradigm for sustaining ecosystem structure and function. *Environ. Sci Technol.* 33 (10), 1545–1551.
- Robinson, A.P., Froese, R.E., 2004. Model validation using equivalence tests. *Ecol. Model.* 176, 349–358.
- Theil, H., 1966. *Applied economic forecasting*. North-Holland, Amsterdam, the Netherlands.
- Tian, H.Q., Liu, M.L., Zhang, C., Ren, W., Chen, G.S., Xu, X.F., Lv, C.Q., 2005. DLEM-The Dynamic land ecosystem model, user manual, *Ecosystem Dynamics and Global Ecology Lab*. Auburn University, Auburn, AL, USA.
- Tian, H.Q., Chen, G.S., Liu, M.L., Zhang, C., Sun, G., Lu, C.Q., Xu, X.F., Ren, W., Pan, S., Chappelka, A., 2010. Model estimates of net primary productivity, evapotranspiration, and water use efficiency in the terrestrial ecosystems of the southern United States during 1895–2007. *For. Ecol. Manag.*, doi:10.1016/j.foreco.2009.10.0009.
- Tian, H.Q., Xu, X.F., 2007. Process-based ecosystem modeling in support of the FIRE Project. Final PO Report to South Florida Water Management District, West Palm Beach, FL, USA.
- Urban, N.H., Davis, S.M., Aumen, N.G., 1993. Fluctuations in sawgrass and cattail densities in Everglades Water Conservation Area 2A under varying nutrient, hydrologic and fire regimes. *Aquat. Bot.* 46, 203–223.
- Wang, N.M., Mitsch, W.J., 2000. A detailed ecosystem model of phosphorus dynamics in created riparian wetlands. *Ecol. Model.* 126, 101–130.
- Wang, Y.P., Houlton, B.Z., Field, C.B., 2007. A model of biogeochemical cycles of carbon, nitrogen, and phosphorus including symbiotic nitrogen fixation and phosphatase production. *Global Biogeochem. Cy.* 21, GB1018, doi:10.1029/2006GB002797.
- Wellek, S., 2003. *Testing statistical hypothesis of equivalence*. Chapman and Hall, London, U.K.
- Wetzel, R.G., 2001. *Limnology: Lake and River Ecosystems*. Academic Press, San Diego, CA, USA.
- Wu, Y., Sklar, F.H., Gopu, K., Rutchey, K., 1993. Fire simulations in the Everglades Landscape using parallel programming. *Ecol. Model.* 93, 113–124.
- Wynn, T.M., Liehr, S.K., 2001. Development of a constructed subsurface-flow wetland simulation model. *Ecol. Eng.* 16, 519–536.
- Vanclay, J.K., Skovsgaard, J.P., 1997. Evaluating forest growth models. *Ecol. Model.* 98, 1–12.
- Xu, X.F., Tian, H.Q., Miao, S.L., Sindhoj, E., 2008. Effects of fire on phosphorus dynamics and cattail growth in a nutrient-enriched Everglades wetland as simulated by the Wetland Ecosystem Model. In: *ESA 93rd Annual Meeting*, 3–8 August, 2008. Milwaukee, WI, USA.
- Zedler, J.B., 2000. Progress in wetland restoration ecology. *Trends Ecol. Evol.* 15, 402–407.
- Zhang, Y., Li, C.S., Trettin, C.C., Li, H.B., Sun, G., 2002. An integrated model of soil, hydrology, and vegetation for carbon dynamics in wetland ecosystems. *Global Biogeochem. Cy.* 16 (4), 1061, doi:10.1029/2001GB001838.